Time Dimensional Consistency Aware Analysis of Voltage Mode and Current Mode Active Fractional Circuits

Rawid Banchuin[1] and **Roungsan Chaisricharoen**[2]

ABSTRACT

In this research, the analysis of the active fractional circuits has been performed by using the fractional differential equation approach. Both voltage and current mode circuits have been taken into account. The fractional time component parameters have been included in the derivative terms within the fractional differential equations. This is because the consistency in time dimension between the fractional derivative and the conventional one, which is also related to the physical measurability, is concerned. The fractional derivatives have been interpreted in the Caputo sense. The resulting analytical solutions of the time dimensional consistency aware fractional differential equations have been determined. We have found that the dimensional consistency between both sides of the equations of the solutions, which cannot be achieved in the previous works, can be obtained. By applying different source terms to the obtained analytical solutions, the response of both voltage and current mode circuits have been determined and the behaviours of the circuits have been analysed. The fractional time constant and pole locations in the F-plane of these circuits have been determined. Their dynamic behaviours and stabilities have been analysed. Moreover, the discussion on circuit realizations with a fractional capacitor has also been made.

Keywords: Active Fractional Circuit, Current Mode, Fractional Time Component Parameter, Time Dimensional Consistency, Voltage Mode

1. INTRODUCTION

The fractional calculus, which is an extension of the conventional integer calculus, has been extensively utilized in various engineering fields such as robotics [1]-[3], bioengineering [4], [5], electronics [6], [7], signal processing [8], [9] and control theory [10], [11] etc. Its related differential equation, namely fractional differential equation (FDE), has also been widely used in these areas and plays a fundamental role in the fractional order circuit and system [12]-[18] which is a generalization of the classical integer order counterpart. It has been used in the analysis of both active and passive fractional circuits [19]-[23]. However, the time dimension of the fractional derivative terms of these works are not consistent with that of the conventional derivative and also are not physically measurable as they are generically given by $\sec^{-\gamma}$ where γ can be non-integer. On the other hand, that of the conventional derivative is given by sec-1, which in turn is physically measurable. Fortunately, the fractional time component parameter has been introduced in the previous work on fractional mechanical systems [24]. By including such a parameter in the fractional derivative term, the time dimension of the fractional derivative term with this new parameter becomes $\sec^{-1}$. This motivates electrical engineers to apply the fractional time component parameter included fractional derivative in the analyses of passive fractional circuits [25][26] which are electrical systems, for obtaining the time dimensional consistency to the conventional derivative. However, similar analysis of active fractional circuits has never been performed, despite the previous attempts to analyse the active fractional circuits with FDE [22], [23].

Hence, the analysis of the active fractional circuits with the awareness of such time dimensional consistency has been performed in this work by using the FDE based approach. The fractional time component has been incorporated into the fractional derivative terms for obtaining the time dimensional consistency for the conventional derivative. Since any active circuit can be classified as either a voltage mode circuit or a current mode circuit by using its transfer function [27] [28], both voltage and current mode circuits have been analysed in this work. This is unlike [22], which considered only the voltage mode circuit. Here, the OPAMP and CC based fractional order filters has been respectively adopted for the candidate voltage and current mode active fractional circuit. Both OPAMP and CC have been often cited for decades, and these circuits purely operate in the voltage and current mode. This is in contrast to the OTA-C fractional order filter adopted in [23], which takes the voltage as the input and produces the output current. Moreover, more complicated voltage and current mode active fractional circuits can be designed

Manuscript received on May 10, 2018 ; revised on March 25, 2019.
Final manuscript received on April 20, 2019.
[1] The author is with Graduated school of IT and Faculty of Engineering, Siam University, Bangkok, Thailand, E-mail: rawid_b@yahoo.com
[2] The author is with School of IT, Mae Fah Luang University, Chiangrai, Thailand, E-mail: roungsan.cha@mfu.ac.th

by using our candidate circuits as the basic building blocks. The fractional time component parameter included fractional derivative terms of the FDEs have been defined in the Caputo sense [29] due to its simplicity in determining its Laplace transform and its real world modelling advantages [30]. The analytical solutions of the formulated FDEs, which have been determined by using the Laplace-inverse Laplace transformation [31] based methodology, employ the dimensional consistency between both sides of their equations. This consistecy does not exist in the solutions proposed in those previous works which ignored time dimensional consistency [19]-[23]. By applying different source terms, including the AC sources, to the obtained solutions, the response of both voltage and current mode circuits have been determined and the behaviours of the circuits have been analysed. Moreover, we determine the fractional time constants [25] and the pole locations in the F-plane of these circuits. We also analyse their dynamic behaviours and stabilities. Therefore more detailed analysis of the active fractional circuit compared to those of [22] and [23] is presented. It should be mentioned here that the proposed analysis results can serve as a basis for understanding, analysis, and design of those more complicated fractional voltage and current mode active circuits. They can be realized by using our candidate circuits as the basic building blocks as stated above. Any system can be well understood by understanding as of its fundamental building blocks. For example, it is obvious that any system with order 3 or higher can be well understood by using the understanding on the 1st and 2nd order systems as the basis. Apart from those aforementioned studies, the realizations of both voltage and current mode active fractional circuits by using the state of the art fractional capacitor will be discussed.

2. AN OVERVIEW OF FRACTIONAL DERIVATIVE

Before proceeding further, an overview of fractional derivative, which is the main component of the FDE, will be briefly given. Unlike the conventional derivative, the order of the fractional derivative can be fractional. There exist various mathematical definitions of the fractional derivative, e.g. the Riemann-Liouvielle definition and the Caputo definition, etc. Let $x(t)$ be an arbitrary time domain function. Its fractional derivative of arbitrary order is denoted by α and is $\frac{d^\alpha}{dt^\alpha}x(t)$, where $0 < \alpha \leq 1$ can be given in terms of the conventional derivative and an integral using the Riemann-Liouvielle definition as shown in equation 1.

$$\frac{d^\alpha}{dt^\alpha}x(t) = \frac{d}{dt}[X(t,\alpha)] \tag{1}$$

$X(t,\alpha)$ denotes the fractional integral of $x(t)$ of order α which can be given by equation 2.

$$X(t,\alpha) = \frac{1}{\Gamma(1-\alpha)}\int_0^t (t-\tau)^{-\alpha}x(\tau)d\tau \tag{2}$$

Noted that $\Gamma()$ stands for the gamma function [32] which can be recursively defined in term of arbitrary value, x, as given by equation 3.

$$\Gamma(x+1) = x\Gamma(x) \tag{3}$$

On the other hand, $\frac{d^\alpha}{dt^\alpha}x(t)$ can be given using the Caputo definition as follows:

$$\frac{d^\alpha}{dt^\alpha}x(t) = \frac{1}{\Gamma(1-\alpha)}\int_0^t \frac{x'(\tau)}{(t-\tau)^\alpha}d\tau \tag{4}$$

where

$$x'(t) = \frac{d}{dt}x(t) \tag{5}$$

If the Riemann-Liouvielle definition has been assumed, the Laplace transform of $\frac{d^\alpha}{dt^\alpha}x(t)$ can be given by

$$L[\frac{d^\alpha}{dt^\alpha}x(t)] = s^\alpha X(s) - X(0,1-\alpha) \tag{6}$$

where

$$X(0,1-\alpha) = \frac{1}{\Gamma(-\alpha)}\int_{0^+}^t (t-\tau)^{-(1-\alpha)}x(\tau)d\tau\big|_{t=0} \tag{7}$$

Alternatively, if we defined $\frac{d^\alpha}{dt^\alpha}x(t)$ in the Caputo sense, we have

$$L[\frac{d^\alpha}{dt^\alpha}x(t)] = s^\alpha X(s) - s^{\alpha-1}x(0) \tag{8}$$

which is much simpler than that obtained by using the Riemann-Liouvielle definition. This is because $x(0)$, which stands for the initial value of $x(t)$, can be immediately applied similarly to the Laplace transformation of the conventional derivative without any necessity to perform the fractional integral as given by (7) if the Riemann-Liouvielle definition has been adopted. Moreover, unlike the Caputo definition, the Riemann-Liouvielle definition also has certain mathematical flaws. These include nonzero derivative of a constant, derivative with one or more singular points of an analytic function, and complex valued derivative of a real valued function [30]. It can be stated that the Caputo definition has real world modelling advantages over that of Riemann-Liouvielle. Because of this advantage and the simplicity in finding the Laplace transform as mentioned above, we adopt the

Caputo definition for our work.

3. ANALYSIS OF THE VOLTAGE MODE ACTIVE FRACTIONAL CIRCUIT

In this section, the analysis of the voltage mode active fractional circuit will be performed by using the OPAMP based fractional filter as our candidate circuit as aforementioned. Such a candidate circuit can be constructed by using the OPAMP based conventional filter [22] [33] which is depicted in Fig.1 as the basis.

To begin, the FDE of our candidate voltage mode circuit must be formulated. In order to do so, the voltage transfer function, $H_v(s)$, of its basis, the OPAMP based conventional filter, must be determined first. This is because it is convenient to perform the analysis of any fractional circuit by starting from its conventional prototype and then extend the obtained results toward the fractional circuit of interest. Such an approach has been widely adopted in the aforesaid previous works on analyses of fractional circuits [19]-[23] [26]. By using conventional circuit analysis, we obtain the following voltage transfer function

$$H_v(s) = \frac{(1 + (R_2/R_1))/RC}{s + (1/RC)} \tag{9}$$

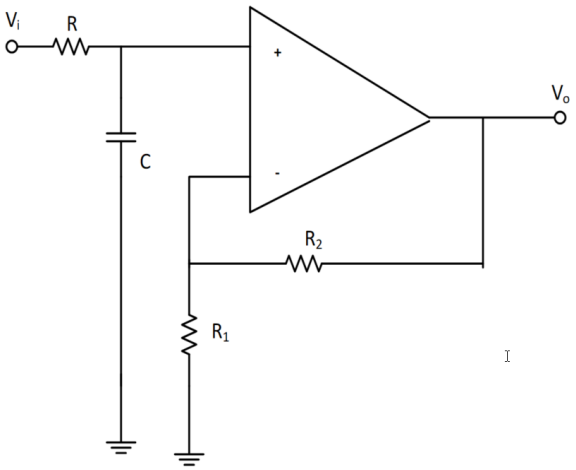

Fig.1: *The OPAMP based conventional filter [22], [33].*

By using (9) and the definition of $H_v(s)$, the relationship between $v_i(t)$ and $v_o(t)$, which respectively denote the source and output voltage, can be obtained in terms of an ordinary differential equation (ODE) as follows [22]:

$$\frac{d}{dt}v_o(t) + \frac{1}{RC}v_o(t) = \frac{1 + (R_2/R1)}{RC}v_i(t) \tag{10}$$

For obtaining the desired FDE, the conventional time derivative, i.e. $\frac{d}{dt}$, in (10) must be replaced by the fractional one. Unlike [22], the fractional time component parameter has been taken into account for obtaining the time dimensional consistency. As a result, the time dimensional consistency aware FDE of the OPAMP based fractional filter can be formulated as follows:

$$\sigma_v^{\alpha-1}\frac{d^\alpha}{dt^\alpha}v_o(t) + \frac{1}{RC}v_o(t) = \frac{1 + (R_2/R1)}{RC}v_i(t) \tag{11}$$

where σ_v represents the fractional time component parameter of this voltage mode circuit and can range from 0 to RC. Moreover, (11) will be reduced to (10) if we let $\alpha = 1$. Since σ_v has the dimension of sec [24] [25] and the time dimension of $\frac{d^\alpha}{dt^\alpha}$ is given regardless of the definition of the fractional derivative by $\sec^{-\alpha}$, the dimension of the term $\sigma_v^{\alpha-1}\frac{d^\alpha}{dt^\alpha}$, has been found to be $\sec^{-1}$. That is both consistent with that of $\frac{d}{dt}$ and physically measurable as aforesaid.

In order to solve (11), the Laplace transformation must be applied to both sides of the equation. Such Laplace transformation based methodology is applicable as (11) is linear. Since $\frac{d}{dt}$ has been defined in the Caputo sense, the Laplace transform of $\frac{d^\alpha}{dt^\alpha}v_o(t)$ can be given by [29]

$$L[\frac{d^\alpha}{dt^\alpha}v_o(t)] = s^\alpha V_o(s) - s^{\alpha-1}v_o(0) \tag{12}$$

where $v_o(0)$ and $V_o(s)$ denote the initial value of output voltage and such voltage in the s-domain respectively. After taking the Laplace transformation, (11) becomes

$$\sigma_v^{\alpha-1}s^\alpha V_o(s) - v_o(0)\sigma_v^{\alpha-1}s^{\alpha-1} + \frac{1}{RC}V_o(s) = \frac{1 + (R_2/R1)}{RC}V_i(s) \tag{13}$$

As a result, $V_o(s)$ can be given in terms of a function of the s-domain source voltage, $V_i(s)$ as

$$V_o(s) = v_o(0)\left[\frac{s^{\alpha-1}}{s^\alpha + \frac{1}{\sigma^{\alpha-1}RC}}\right] + \frac{(1 + (R_2/R_1))}{\sigma^{\alpha-1}RC}\left[\frac{V_i(s)}{s^\alpha + \frac{1}{\sigma^{\alpha-1}RC}}\right] \tag{14}$$

By using the inverse Laplace transformation and the convolution theorem [31], $v_o(t)$ of the candidate voltage mode active circuit can be analytically determined as follows:

$$v_o(t) = v_o(0)E_\alpha(-\frac{t^\alpha}{\sigma_v^{\alpha-1}RC}) + \frac{(1+(R_2/R_1))}{\sigma^{\alpha-1}RC}[v_i(t) * t^{\alpha-1}E_{\alpha,\alpha}(-\frac{t^\alpha}{\sigma_v^{\alpha-1}RC}) \tag{15}$$

where $*$ denotes the convolution operator. It should be mentioned here that $E_\alpha()$ stands for the Mittag-

Leffler function [32], which can be defined in terms of an arbitrary variable x as

$$E_{\alpha}(x) = \sum_{k=0}^{\infty} \left[\frac{x^k}{\Gamma(\alpha k + 1)} \right] \tag{16}$$

Moreover, $E_{\alpha,\alpha}() = E_{\alpha,\beta}()\big|_{\beta=\alpha}$ where $E_{\alpha,\beta}()$ denotes the generalized Mittag-Leffler function [32], which can be defined for any x as

$$E_{\alpha,\beta}(x) = \sum_{k=0}^{\infty} \left[\frac{x^k}{\Gamma(\alpha k + \beta)} \right] \tag{17}$$

It can be seen from (16) and (17) that $E_{\alpha}(\ ) = E_{\alpha-1}(\ )$. Finally, the convolution operation can be defined for arbitrary functions $f(t)$ and $g(t)$ as follows [31]:

$$f(t) * g(t) = \int_0^t f(\tau) g(t-\tau) d\tau \tag{18}$$

With this definition, (15) becomes

$$\begin{aligned} v_o(t) =& v_o(0) E_{\alpha}(-\frac{t^{\alpha}}{\sigma_v^{\alpha-1} RC}) \\ &+ \frac{(1+(R_2/R_1))}{\sigma_v^{\alpha-1} RC} \int_0^t v_i(\tau)(t-\tau)^{\alpha-1} E_{\alpha,\alpha}[-\frac{(t-\tau)^{\alpha}}{\sigma_v^{\alpha-1} RC}] d\tau \end{aligned} \tag{19}$$

At this point, the analytical solution of the time dimensional consistency aware FDE of the candidate voltage mode active fractional circuit which is the circuit response to arbitrary source term, has been already determined. We have found that the dimensional consistency between both sides of (19) can be obtained since the dimensions of both RHS and LHS are V, due to the effect of σ_v. This is because both $\frac{t^{\alpha}}{\sigma_v^{\alpha-1} RC}$ and $\frac{(t-\tau)^{\alpha}}{\sigma_v^{\alpha-1} RC}$ are dimensionless. Therefore $E_{\alpha}(-\frac{t^{\alpha}}{\sigma_v^{\alpha-1} RC})$ and $E_{\alpha,\alpha}(-\frac{(t-\tau)^{\alpha}}{\sigma_v^{\alpha-1} RC})$ are dimensionless as well since they are respectively the power series of $\frac{t^{\alpha}}{\sigma_v^{\alpha-1} RC}$ and $\frac{(t-\tau)^{\alpha}}{\sigma_v^{\alpha-1} RC}$ as can be seen from (16) and (17). As a result, both terms on the RHS of (19) have the dimension of V which are consistent to that of the LHS, as the dimension of $v(0)$ is V and those of $\frac{(1+(R_2/R_1))}{\sigma_v^{\alpha-1} RC}$ and $\int_0^t v_i(\tau)(t-\tau)^{\alpha-1} E_{\alpha,\alpha}[-\frac{(t-\tau)^{\alpha}}{\sigma_v^{\alpha-1} RC}] d\tau$ are $\text{sec}^{-\alpha}$ and $\text{Vsec}^{-\alpha}$ respectively. It should be mentioned here that the dimensional consistency similar to that of (19) which also achieved by a solution of the time dimensional consistency aware FDE of the candidate current mode active fractional circuit to be presented later, cannot be obtained by those solutions proposed in [19]-[23] because they lack the corresponding fractional time component parameters.

In the following subsections, the circuit responses due to different sources, i.e. zero source, DC source and AC source, will be respectively formulated and the time dimensional consistency aware behavioural analysis of the voltage mode circuit in fractional domain will be presented. Moreover, the pole location on the F-plane and a stability analysis of the circuit will also be shown.

3.1 The response to zero source

The response to zero source voltage i.e. $v_i(t) = 0$, which occurs under the source free condition, will be considered first. By using (19), $v_o(t)$ is simply given by

$$v_o(t) = v_o E_{\alpha}(-\frac{t^{\alpha}}{\sigma_v^{\alpha-1} RC}) \tag{20}$$

By assuming that $\sigma_v = RC$, $C = 1$ μF, $R = 1$ MΩ and $v_o(0) = 1$ V, $v_o(t)$ can be simulated against t under for different values of α as depicted in Fig. 2. It can be seen that the behavior $v_o(t)$ of when α approaches 1 becomes closer to that of the OPAMP based conventional filter which acts as a decreasing exponential function. This is because $E_1(x) = e^x$ [32].

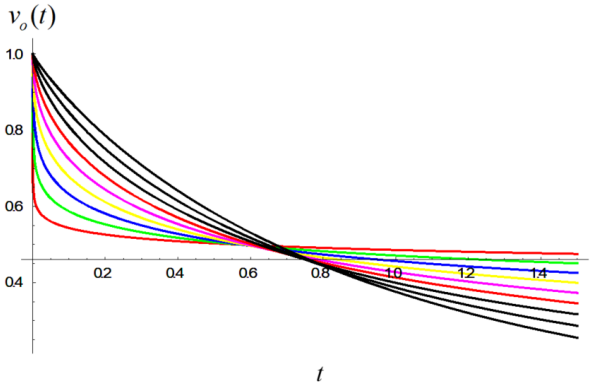

Fig.2: *$v_o(t)$ due to zero source term v.s. t ($\alpha = 0.1$ (red), $\alpha = 0.2$ (green), $\alpha = 0.3$ (blue), $\alpha = 0.4$ (yellow), $\alpha = 0.5$ (pink), $\alpha = 0.6$ (magenta), $\alpha = 0.7$ (black), $\alpha = 0.8$ (brown), $\alpha = 0.9$ (gray)).*

3.2 The response to DC source

Now $v_o(t)$, due to the DC source voltage applied at $t = 0$ which can be mathematically modeled by using the step function as $v_i(t) = Vu$, will be formulated. By using (19), $v_o(t)$ due to such input can be found as

$$v_o(t) = v_o(0)E_\alpha(-\frac{t^\alpha}{\sigma_v^{\alpha-1}RC}) + \frac{(1+(R_2/R_1))}{\sigma_v^{\alpha-1}RC}\int_0^t (t-\tau)^{\alpha-1}E_{\alpha,\alpha}[-\frac{(t-\tau)^\alpha}{\sigma_v^{\alpha-1}RC}]d\tau \quad (21)$$

This is because $u(t) = 1$ for $t \geq 1$. By using (17) with $\beta = \alpha$ and the basic properties of the generalized Mittag-Leffler function [32], it has been found that [22]

$$\int_0^t (t-\tau)^{\alpha-1}E_{\alpha,\alpha}[-\frac{(t-\tau)^\alpha}{\sigma_v^{\alpha-1}RC}]d\tau = -\sigma_v^{\alpha-1}RC[E_\alpha(-\frac{(t-\tau)^\alpha}{\sigma_v^{\alpha-1}RC}) - 1] \quad (22)$$

As a result, $v_o(t)$ can be given by

$$v_o(t) = [v_o(0) - V(1+\frac{R_2}{R_1})]E_\alpha(-\frac{t^\alpha}{\sigma_v^{\alpha-1}RC}) + V(1+\frac{R_2}{R_1}) \quad (23)$$

By assuming extremely small $R_2, R_1 = 1$ MΩ with other conditions but $v_o(0)$ defined similarly to those assumed in the previous subsection, can be simulated against t for different values of α when $V = 1.5$ V and $v_o(0) = 2.5$ V, i.e. $V < v_o(0)/(1 + (R_2/R_1))$ as depicted in Fig. 3. On the other hand, $v_o(t)$'s with $V = 2.5$ V and $v_o(0) = 1.5$ V, i.e. $V > v_o(0)/(1+(R_2/R_1))$ can be simulated as shown in Fig. 4. It can be seen from Fig. 3 that $v_o(t)$ due to the DC input with $V > v_o(0)/(1 + (R_2/R_1))$ behaves very similar to $v_o(t)$ due to zero input. Fig. 4 shows that with $V > v_o(0)/(1+(R_2/R_1))$ becomes an increasing function instead. Moreover, both figures show that $v_o(t)$ with larger α become closer to that of the OPAMP based conventional filter which acts as a decreasing exponential function and an increasing one if we let $V > v_o(0)/(1 + (R_2/R_1))$ and vice versa. If we let $V > v_o(0)/(1 + (R_2/R_1))$, (23) becomes

$$v_o(t) = V(1 + \frac{R_2}{R_1}) \quad (24)$$

which means that the DC output voltage with the magnitude of $V/(1 + (R_2/R_1))$ is obtained for any value of α.

3.3 The response to AC source

By applying the AC source voltage given by $v_i(t) = V\sin(\omega t + \phi)$ to (19), $v_o(t)$ can be found as

$$v_o(t) = v_o(0)E_\alpha(-\frac{t^\alpha}{\sigma_v^{\alpha-1}RC}) + \frac{(1+(R_2/R_1))}{\sigma_v^{\alpha-1}RC}\int_0^t \sin(\omega\tau+\phi)(t-\tau)^{\alpha-1}E_{\alpha,\alpha}[-\frac{(t-\tau)^\alpha}{\sigma_v^{\alpha-1}RC}]d\tau \quad (25)$$

By using (17) with $\beta = \alpha$, (25) becomes

$$v_o(t) = v_o(0)E_\alpha(-\frac{t^\alpha}{\sigma_v^{\alpha-1}RC}) + \frac{(1+(R_2/R_1))}{\sigma_v^{\alpha-1}RC}\int_0^t \sin(\omega\tau+\phi)(t-\tau)^{\alpha-1}\sum_{k=0}^{\infty}\left[\frac{[-\frac{(t-\tau)^\alpha}{\sigma_v^{\alpha-1}RC}]^k}{\Gamma(\alpha k+\alpha)}\right]d\tau \quad (26)$$

After interchanging the summation and integral and performing the integration, $v_o(t)$ due to the AC source term can be finally given as follows:

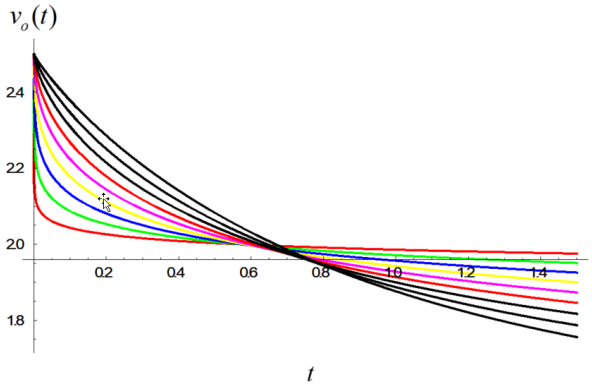

Fig.3: *$v_o(t)$ due to DC source term v.s. t when $V < v_o(0)/(1 + (R_2/R_1))t$ ($\alpha = 0.1$ (red), $\alpha = 0.2$ (green), $\alpha = 0.3$ (blue), $\alpha = 0.4$ (yellow), $\alpha = 0.5$ (pink), $\alpha = 0.6$ (magenta), $\alpha = 0.7$ (black), $\alpha = 0.8$ (brown), $\alpha = 0.9$ (gray)) .*

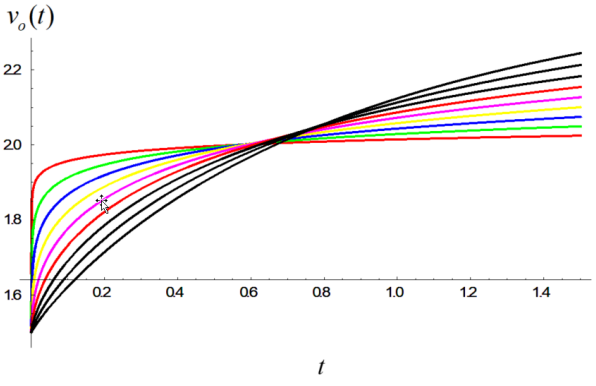

Fig.4: *$v_o(t)$ due to DC source term v.s. t when $V < v_o(0)/(1 + (R_2/R_1))t$ ($\alpha = 0.1$ (red), $\alpha = 0.2$ (green), $\alpha = 0.3$ (blue), $\alpha = 0.4$ (yellow), $\alpha = 0.5$ (pink), $\alpha = 0.6$ (magenta), $\alpha = 0.7$ (black), $\alpha = 0.8$ (brown), $\alpha = 0.9$ (gray)) .*

$$\begin{aligned} v_o(t) =& v_o(0)E_\alpha(-\frac{t^\alpha}{\sigma_v^{\alpha-1}RC}) \\ &- \{\sqrt{\pi}V(1+\frac{R_2}{R_1})[\omega t\cos(\phi) + 2\sin(\phi)] \\ &\times \sum_{k=0}^{\infty}[(-\frac{1}{\sigma_v^{\alpha-1}RC})^{k+1}2^{-\alpha(k+1)}t^{\alpha(k+1)} \\ &\times_1 \tilde{F}_2(1; \frac{1}{2}(\alpha(k+1)+1), \frac{1}{2}(\alpha(k+1)+2); \frac{1}{4}(\omega t)^2)]\} \end{aligned} \quad (27)$$

where

$$\times_1 \tilde{F}_2(1;\frac{1}{2}(\alpha(k+1)+1),\frac{1}{2}(\alpha(k+1)+2);\frac{1}{4}(\omega t)^2)]\}$$
$$=_1 \tilde{F}_2(a_1;b_1,b_2;z)|_{a_1=1,b_1=\frac{1}{2}(\alpha(k+1)+1),b_2=\frac{1}{2}(\alpha(k+1)+2);z=-\frac{1}{4}(\omega t)^2} \quad (28)$$

It should be mentioned here that ${}_1\tilde{F}_2(\ ;\ ,\ ;)$ is the regularized hypergeometric function with $p = 1$ and $q = 2$ [34]. In the general case in which p and q can be positive integers, the regularized hypergeometric function can be defined as [34]

$${}_p\tilde{F}_q(a_1,a_2,\ldots,a_p;b_1,b_2,\ldots,b_q;z)=\frac{{}_pF_q(a_1,a_2,\ldots,a_p;b_1,b_2,\ldots,b_q;z)}{\Gamma(b_1),\Gamma(b_2,\ldots,\Gamma(b_q)} \quad (29)$$

where ${}_pF_q(\ ;\ ,\ ;)$ denotes the generalized hypergeometric function with arbitrary p and q, which in turn can be defined as a series which converges if and only if $p \leq q$ as [35]

$${}_pF_q(a_1,a_2,\ldots,a_p;b_1,b_2,\ldots,b_q;z)=\sum_{n=0}^{\infty}[\frac{\prod_{i=1}^{p}(a_i)_n}{\prod_{j=1}^{q}(b_{jn})}\frac{z^n}{n!}] \quad (30)$$

where (a_i)n and (b_j)n are Pochhammer symbols which can be respectively defined as

$$(a_i)_n=(a_i)(a_i+1)(a_i+n-1)=\frac{\Gamma(a_i+n)}{\Gamma(a_i)} \quad (31)$$

$$(b_j)_n=(b_i)(b_j+1)(b_j+n-1)=\frac{\Gamma(b_j+n)}{\Gamma(b_j)} \quad (32)$$

By assuming that $v_o(0) = 0$ and $v_i(t)$ employs $\omega = 10^6\pi$ rad/s, which is obviously high, $\phi = 0$ rad and $V = 1$ V, $v_o(t)$ can be simulated against t and α under the other conditions similar to those adopted in the previous subsections as depicted in Fig.5, which shows that the magnitude of $v_o(t)$ is inversely proportional to α.

3.4 The fractional time constant and the dynamic analysis

By carefully considering (23), $v_o(t)$ due to DC source voltage can be given in an alternative manner as follows

$$v_o(t)=[v_o(0)-V(1+\frac{R_2}{R_1})]E_\alpha(-\frac{t^\alpha}{T_{v\alpha}})+V(1+\frac{R_2}{R_1}) \quad (33)$$

where

$$T_{v\alpha}=\sigma_v^{\alpha-1}RC \quad (34)$$

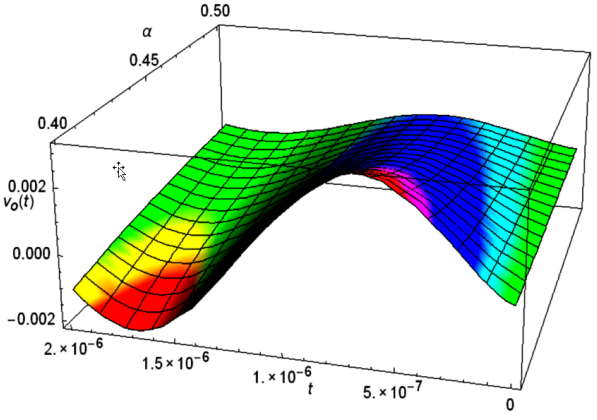

Fig.5: *$v_o(t)$ due to AC source term v.s. t and α.*

According to [25], $T_{\alpha v}$ stands for the fractional time constant of the candidate voltage mode active fractional circuit. It determines the dynamic of such a circuit as it is defined as the time instant where $v_o(t)$ due to DC source with $V > v_o(0)/(1+(R_2/R_1))$ rises to approximately 63.2% of its final value.

Since the time constant of the OPAMP based conventional filter can be given by $T_v = RC$, we have

$$T_{v\alpha}=\sigma_v^{\alpha-1}T_v \quad (35)$$

From Fig. 4, it can be clearly seen that such $v_o(t)$ with lower α rises to approximately 63.2% of its final value with a faster rate. Therefore we can imply here that $T_{\alpha v}$ is inversely proportional to α which means that the voltage mode circuit with lower α is more responsive to the stimulus. Since $0 < \alpha \leq 1$, it can be seen from (35) that $T_{\alpha v}$ is inversely proportional to α, thus a similar implication can be made.

3.5 The pole location on the F-plane and the stability analysis

For studying the stability of any linear fractional system, its pole location on either the F-plane or W-plane must be determined as the applicability of s-plane ceases to be valid [13], [36]. These planes can be respectively depicted in Fig. 6 and 7 where m can be arbitrary positive integer. From these figures, it can be seen that the unstable areas of both the F-plane and the W-plane are smaller than that of the s-plane, which implies that the fractional system has a better chance of stability than the conventional integer system. In order to find such pole locations, the characteristic equation of the system obtained from its transfer function must be formulated first.

By using (14), which can be obtained by taking the Laplace transformation to both sides of the time dimensional measurability aware FDE of the candidate voltage mode active fractional circuit (11), as aforesaid, the transfer function given by (36) can be obtained

$$H_v(s^\alpha) = \frac{(1+(R_2/R_1))/\sigma_v^{\alpha-1}RC}{s^\alpha + \frac{1}{\sigma_v^{\alpha-1}RC}} \quad (36)$$

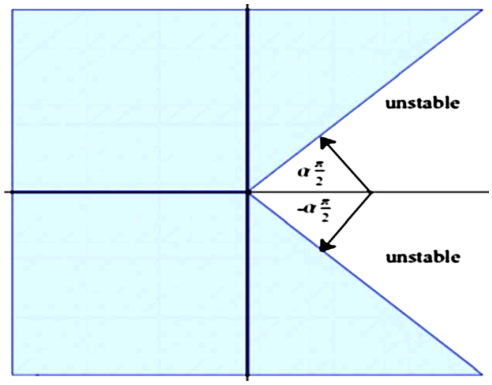

Fig.6: *The F-plane [36].*

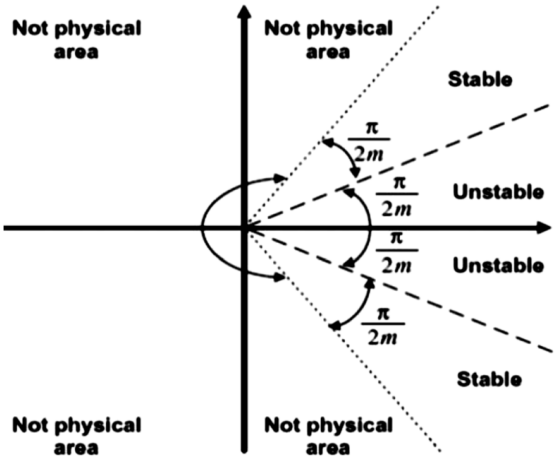

Fig.7: *The W-plane [30].*

$$s^\alpha + \frac{1}{\sigma_v^{\alpha-1}RC} = 0 \quad (37)$$

Since the left hand side of (30) can be written in the form $\sum_{k=0}^{m} a_k s^{k\alpha}$ where k is a positive integer, the F-plane based stability analysis has been found to be suitable [13]. Noted that k can be 0 and 1 and $a_0 = 1/\sigma_v^{\alpha-1}RC$ and $a_1 = 1$ in this scenario. By simply replacing s? by the fractional power complex variable F, (37) becomes

$$F + \frac{1}{\sigma_v^{\alpha-1}RC} = 0 \quad (38)$$

and thus we have

$$F = -\frac{1}{\sigma_v^{\alpha-1}RC} \quad (39)$$

Since R, C and σ_v are positive real quantities, it can seen from (39) that F is a negative real. Thus, the circuit pole is located on the negative real axis of the F-plane. From Fig. 6, it can be seen that the area of the unstable region which is α dependent can range from merely the positive real axis to the entire right hand side of the F-plane in this scenario as we assumed that α can range from 0 to 1. Therefore our voltage mode circuit is always stable as its pole will always be in the stable region of the F-plane.

Alternatively, F can be given in the polar form as follows

$$F = \frac{1}{\sigma_v^{\alpha-1}RC}\exp[j\pi] \quad (40)$$

This means that the phase angle of the circuit pole is π rad. As a result, our candidate voltage mode circuit is always stable under the assumed range of α according to the F-plane stability criterion mentioned in [36].

4. ANALYSIS OF THE CURRENT MODE ACTIVE FRACTIONAL CIRCUIT

As stated above, the CC-based fractional filter has been adopted as the candidate current mode active fractional circuit. This circuit can be constructed by generalizing the CC-based conventional filter depicted in Fig. 8, where both CC with single output and dual output have been used.

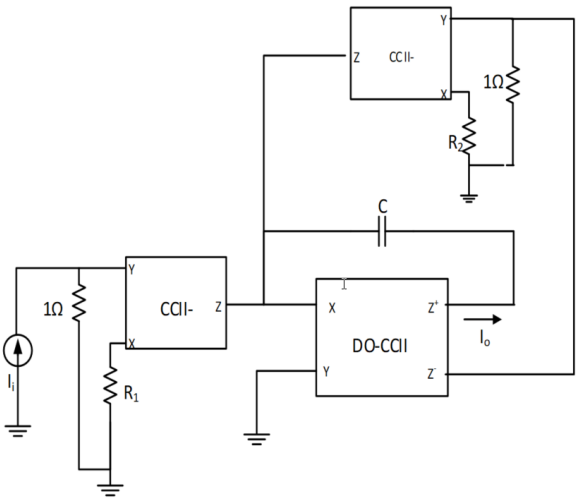

Fig.8: *The CC-based conventional filter.*

Similarly to the voltage mode circuit, we will perform the analysis of the fractional current mode circuit by starting from its conventional prototype and then extending the results toward the fractional circuit. From Fig. 8, it can be seen that the current transfer function, $H_i(s)$ of the CC-based conventional filter can be given by

$$H_i(s) = -\frac{1/R_1C}{s + (1/R_2C)} \quad (41)$$

By using (41) and the definition of $H_i(s)$, we have

$$\frac{d}{dt}i_o(t) + \frac{1}{R_2C}i_o(t) = -\frac{1}{R_1C}i_i(t) \tag{42}$$

where $i_i(t)$ and $i_o(t)$ stand for source and output current.

Therefore the time dimensional consistency aware FDE of our candidate current mode active fractional circuit can be given as follows

$$\sigma_i^{\alpha-1}\frac{d^\alpha}{dt^\alpha}i_o(t) + \frac{1}{R_2C}i_o(t) = -\frac{1}{R_1C}i_i(t) \tag{43}$$

where σ_i denotes the fractional time component parameter in this scenario and can range from 0 to R_2C.

Since the time dimension of σ_i is also given by sec [24], [25] as well as that of σ_v, the time dimension $\sigma_i^{\alpha-1}\frac{d^\alpha}{dt^\alpha}$ is given by sec-1. By using the Laplace transformation based methodology and the convolution theorem, $i_o(t)$ of the candidate current mode active circuit can be analytically determined as follows

$$i_o(t) = i_o(0)E_\alpha(-\frac{t^\alpha}{\sigma_i^{\alpha-1}R_2C}) - \frac{\sigma_i^{1-\alpha}}{R_1C}\int_0^t i_i(\tau)(t-\tau)^{\alpha-1}E_{\alpha,\alpha}[-\frac{(t-\tau)^\alpha}{\sigma_i^{\alpha-1}R_2C}]d\tau \tag{44}$$

where $i_o(0)$ stand for the initial value of $i_o(t)$.

At this point, the time dimensional consistent analytical solution of the FDE of the candidate current mode active fractional circuit, which is the circuit response due to arbitrary source current term, has been already determined. Similarly to the voltage mode circuit, the responses of this current mode circuit due to different source terms, i.e. zero source, DC source and AC source, can be formulated by using the derived solution as will be shown in the subsequent subsections where the F-plane based stability analysis of the circuit will be performed as well.

Before proceeding further, it can be stated that both sides of (44) have dimensional consistency. That is their dimensions are both A due to the effect of σ_i. This is not surprising as both $\frac{t^\alpha}{\sigma_i^{\alpha-1}R_2C}$ and $\frac{(t-\tau)^\alpha}{\sigma_i^{\alpha-1}R_2C}$ are dimensionless. Therefore $E_\alpha(-\frac{t^\alpha}{\sigma_i^{\alpha-1}R_2C})$ and $E_{\alpha,\alpha}[-\frac{(t-\tau)^\alpha}{\sigma_i^{\alpha-1}R_2C}]$are dimensionless as well. As a result, both terms on the RHS of (44) have the dimensions of A which are consistent to that of the LHS, as the dimension of $i(0)$ is A and those of $\frac{\sigma_i^{i-\alpha}}{R_1C}$ and $\int_0^t i_i(\tau)(t-\tau)^{\alpha-1}E_{\alpha,\alpha}[-\frac{(t-\tau)^\alpha}{\sigma_i^{\alpha-1}R_2C}]d\tau$ are $\sec^{-\alpha}$ and A secα respectively.

4.1 The response to zero source

By letting $i_i(t) = 0$ in (40), $i_o(t)$ can be simply given by

$$i_o(t) = i_o(0)E_\alpha(-\frac{t^\alpha}{\sigma_i^{\alpha-1}R_2C}) \tag{45}$$

and can be simulated against t under the assumption that $\sigma_i = R_2C, C = 1$ μF, $R_2 = 1$ MΩ and $i_o(0) = 1$ A for different values of α as depicted in Fig. 9. Similarly to $v_o(t)$ of the voltage mode circuit, $i_o(t)$ also become closer to that of the CC-based conventional filter, which also acts as a decreasing exponential function, when α approaches 1 for similar mathematical reasons.

4.2 The response to DC source

Now $i_o(t)$ due to the DC source current applied at $t = 0$ will be formulated. By substituting $i_i(t) = Iu(t)$ in (44), $i_o(t)$ due to the DC source current can be found as

$$i_o(t) = i_o(0)E_\alpha(-\frac{t^\alpha}{\sigma_i^{\alpha-1}R_2C}) - \frac{\sigma_i^{1-\alpha}I}{R_1C}\int_0^t (t-\tau)^{\alpha-1}E_{\alpha,\alpha}[-\frac{(t-\tau)^\alpha}{\sigma_i^{\alpha-1}R_2C}]d\tau \tag{46}$$

After performing the integration with the aid of (10) and the basic properties of the generalized Mittag-Leffler function, (46) becomes

$$i_o(t) = [i_o(0) + \frac{R_2I}{R_1}]E_\alpha(-\frac{t^\alpha}{\alpha_i^{\alpha-1}R_2C}) - \frac{R_2I}{R_1} \tag{47}$$

By using a similar assumption to those of the previous subsection but with $R_1 = 1$ MΩ, $i_o(0) = 1.5$ A and $I = 0.5$ A, this $i_o(t)$ can be simulated against t for different values of α as depicted in Fig. 10. Noted that $I > R_1i_o(0)/R_2$ is satisfied in this scenario and $i_o(t)$ with opposite dynamic can be expected if $I < R_1i_o(0)/R_2$. It can be seen that due to DC source also becomes closer to that of the CC-based conventional filter which behaves like a decreasing exponential function, when α approaches 1.

4.3 The response to the AC source

By applying the AC source current given by $i_i(t) = I\sin(\omega t + \phi)$ to (44), $i_o(t)$ can be found as

$$i_o(t) = i_o(0)E_\alpha(-\frac{t^\alpha}{\sigma_i^{\alpha-1}R_2C}) - \frac{\sigma_i^{1-\alpha}I}{R_1C}\int_0^t \sin(\omega\tau+\phi)(t-\tau)^{\alpha-1}E_{\alpha,\alpha}[-\frac{(t-\tau)^\alpha}{\sigma_i^{\alpha-1}R_2C}]d\tau \tag{48}$$

By using (17) for defining the Mittag-Leffler function and performing the integration, $i_o(t)$ due to the AC source term can be finally given in (49). Moreover, if we adopt similar assumptions to those of the previous subsection but with $i_o(0) = 0$ A, and we also assume that $i_i(t)$ employs $\omega = 10^6\pi$ rad/s, $\phi = 0$ rad and $I = 1$ A has a very high frequency with unity magnitude and zero phase shift, $i_o(t)$ can be simulated against t and α as depicted in Fig. 11, which

shows that the magnitude of $i_o(t)$ are also inversely proportional to α. This behavior of is similar to that of $i_o(t)$ due to AC source depicted in Fig. 5. However, it can be seen that the phase shift of $i_o(t)$ is 180°, which means that $i_o(t)$ is 180° out of phase to $i_i(t)$. This is unlike $v_o(t)$ due to AC source being in phase with $v_i(t)$.

$$\begin{aligned} i_o(t) =& i_o(0)E_\alpha(-\frac{t^\alpha}{\sigma_v^{\alpha-1}RC}) \\ & - \{\sqrt{\pi}(\frac{R_2 I}{R_1})[\omega t\cos(\phi)+2\sin(\phi)] \\ & \times \sum_{k=0}^{\infty}[(-\frac{1}{\sigma_v^{\alpha-1}RC})^{k+1}2^{-\alpha(k+1)}t^{\alpha(k+1)} \\ & \times_1 \tilde{F}_2(1;\frac{1}{2}(\alpha(k+1)+1),\frac{1}{2}(\alpha(k+1)+2);\frac{1}{4}(\omega t)^2)]\} \end{aligned} \tag{49}$$

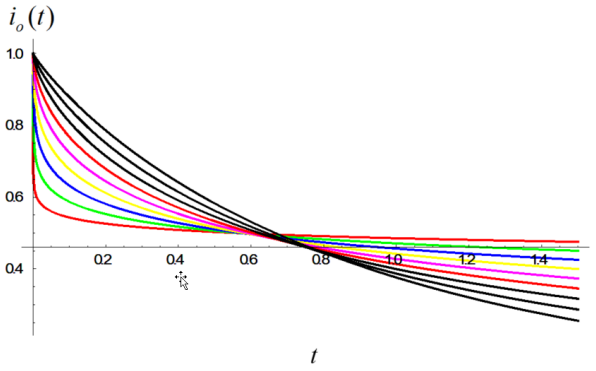

Fig.9: *$i_o(t)$ due to zero source term v.s. t t (α = 0.1 (red), α = 0.2 (green), α = 0.3 (blue), α = 0.4 (yellow), α = 0.5 (pink), α = 0.6 (magenta), α = 0.7 (black), α = 0.8 (brown), α = 0.9 (gray)).*

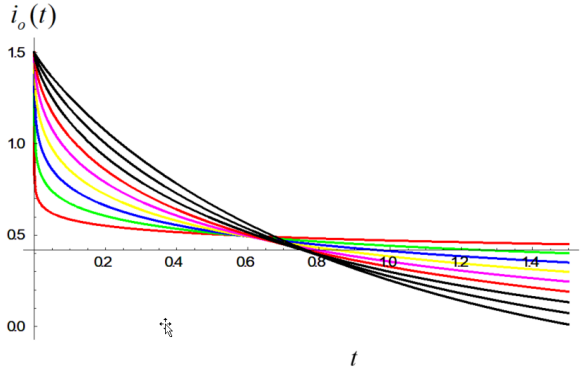

Fig.10: *$i_o(t)$ due to DC source term v.s. t t (α = 0.1 (red), α = 0.2 (green), α = 0.3 (blue), α = 0.4 (yellow), α = 0.5 (pink), α = 0.6 (magenta), α = 0.7 (black), α = 0.8 (brown), α = 0.9 (gray)).*

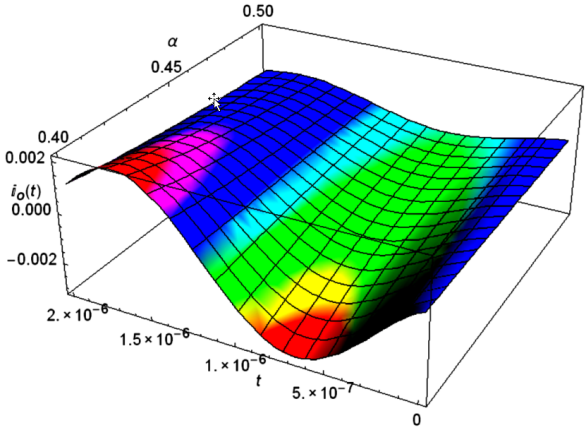

Fig.11: *$i_o(t)$ due to AC source term v.s. t and α.*

4.4 The fractional time constant and the dynamic analysis

By considering (47), $i_o(t)$ due to DC source current can be alternatively given as follows:

$$i_o(t) = [i_o(0) + \frac{R_2 I}{R_1}]E_\alpha(-\frac{t^\alpha}{T_{i\alpha}}) - \frac{R_2 I}{R_1} \tag{50}$$

where

$$T_{i\alpha} = \sigma_i^{\alpha-1}R_2 C \tag{51}$$

Also according to [25], $T_{i\alpha}$ stands for the fractional time constant of the candidate current mode active fractional circuit.

Since the time constant of the CC-based conventional filter can be given by $T_i = R_2 C$, $T_{i\alpha}$ can be alternatively given by

$$T_{i\alpha} = \sigma_i^{\alpha-1}T_i \tag{52}$$

and $0 < \alpha \leq 1$. It can be seen from (52) that $T_{i\alpha}$ is inversely proportional to α. Therefore it can be implied that the current mode circuit with lower α is more responsive to the input.

4.5 The pole location on the F-plane and the stability analysis

For this current mode active fractional circuit, its time dimensional measurability aware transfer function can be obtained by using (39) as

$$H_i(s^\alpha) = \frac{-1/\sigma_i^{\alpha-1}R_1 C}{s^\alpha + \dfrac{1}{\sigma_i^{\alpha-1}R_2 C}} \tag{53}$$

Thus the characteristic equation can be given by

$$s^\alpha + \frac{1}{\sigma_v^{\alpha-1}RC} \tag{54}$$

which is also in terms of $\sum_{k=0}^{m} a_k s^{k\alpha}$. Therefore the F-plane based stability analysis has also been found to be suitable in this scenario where k can also be 0 and 1 and a_1 is also 1. Unlike the active mode fractional circuit, we have found that $a_0 = 1/\sigma_i^{\alpha-1}R_2 C$.

By also simply replacing s^α in (54) by F, we have

$$F = -\frac{1}{\sigma_i^{\alpha-1} R_2 C} \tag{55}$$

As R_2, C, and σ_i are positive real quantities, F is a negative real, thus the pole of the candidate current mode circuit is also located on the negative real axis of the F-plane. Therefore this circuit is also always stable under our assumed range of α for a similar reason to that of the voltage mode active fractional circuit. Moreover, (51) can be rewritten in the polar form as

$$F = -\frac{1}{\sigma_i^{\alpha-1} R_2 C} \exp[j\pi] \tag{56}$$

which means that the phase angle of the pole of the current mode circuit is also π rad. Therefore it is also stable, according to the similar stability criterion, to that of the voltage mode circuit.

5. THE FRACTIONAL CAPACITOR BASED REALIZATION

Both voltage mode and current mode fractional circuits can be realized by simply replacing the conventional capacitor in their corresponding conventional circuit prototypes by a fractional capacitor [37][38]. The fractional capacitor, which is a state of the art electronic device, can be constructed by many means, e.g. ferroelectric material [37], multiwall carbon nanotube (MWCNT)-epoxy nano composite material [38], RC circuit based emulation in the integer domain [39][40] and active device based emulation [7]. According to [41] but in the context of this work, we can define

$$C_\alpha = \sigma^{\alpha-1} C \tag{57}$$

where C_α stands for the pseudo capacitance of the fractional capacitor and employs the dimension of F·sec^{-1} [42]. Note also that σ can be either σ_v or σ_i depending on mode of the circuit under consideration.

By using the definition of C_α and (11), the FDE of our voltage mode fractional circuit realized by using a fractional capacitor is calculated as follows:

$$\frac{d^\alpha}{dt^\alpha} v_o(t) + \frac{1}{RC_\alpha} v_o(t) = \frac{1 + (R_2/R_1)}{RC_\alpha} v_i(t) \tag{58}$$

Therefore we have

$$\begin{aligned} v_o(t) =& v_o(0) E_\alpha(-\frac{t^\alpha}{RC_\alpha}) \\ &+ \frac{(1 + (R_2/R_1))}{RC_\alpha} \int_0^t v_i(\tau)(t-\tau)^{\alpha-1} E_{\alpha,\alpha}[-\frac{(t-\tau)^\alpha}{RC_\alpha}] d\tau \end{aligned} \tag{59}$$

If we let the circuit be supplied by the DC source, the following $v_o(t)$ can be obtained

$$v_o(t) = [v_o(0) - V(1 + \frac{R_2}{R_1})] E_\alpha(-\frac{t^\alpha}{RC_\alpha}) + V(1 + \frac{R_2}{R_1}) \tag{60}$$

By assuming extremely small R_2, $R = R_1 = 1$ MΩ, $V = 1$ V and $v_o(0) = 0$ V, $v_o(t)$'s can be simulated as depicted in Fig. 12. Fractional capacitors with 3 different thickness of coating of PMMA (polymethyl methaacrylate) film on the electrode, t_{PMMA} i.e. $t_{PMMA} = 3$ μm, $t_{PMMA} = 4$ μm and $t_{PMMA} = 6$ μm, [43] have been assumed. As a result, 's with different characteristics can be observed where it has been found that the magnitude of is inversely proportional to t_{PMMA}. Noted that C_α of these practical fractional capacitors are 419.6 F?sec?-1, 468.9 F·sec^{-1} and 616.7 F·sec^{-1}. On the other hand, α are respectively 0.09, 0.11 and 0.12 [43].

For the current mode fractional circuit on the other hand, the FDE of its realization by the using fractional capacitor can be obtained by using (43) and (57) as follows

$$\frac{d^\alpha}{dt^\alpha} i_o(t) + \frac{1}{R_2 C_\alpha} i_o(t) = -\frac{1}{R_1 C_\alpha} i_i(t) \tag{61}$$

Therefore we have

$$i_o(t) = i_o(0) E_\alpha(-\frac{t^\alpha}{R_2 C_\alpha}) - \frac{1}{R_1 C_\alpha} \int_0^t i_i(\tau)(t-\tau)^{\alpha-1} E_{\alpha,\alpha}[-\frac{(t-\tau)^\alpha}{R_2 C_\alpha}] d\tau \tag{62}$$

If we let the circuit be supplied by the DC source, the following $i_o(t)$ can be obtained

$$i_o(t) = [i_o(0) + \frac{R_2 I}{R_1}] E_\alpha(-\frac{t^\alpha}{R_2 C_\alpha}) - \frac{R_2 I}{R_1} \tag{63}$$

By assuming $R_1 = R_2 = 1$ MΩ, I = 1 A and $i_o(0)$ = 1 A, $i_o(t)$'s can be simulated as depicted in Fig. 13 where the fractional capacitors with $t_{PMMA} = 3$ μm, $t_{PMMA} = 4$ μm and $t_{PMMA} = 6$ μm have been assumed. The $i_o(t)$'s with different characteristics can be observed. It has been found that the magnitude of $i_o(t)$ is directly proportional to t_{PMMA}.

6. CONCLUSION

The analysis of both voltage and current mode active fractional circuits has been performed in this research by formulating and analytically solving their FDEs. The OPAMP and CC-based fractional filters have been respectively adopted as the candidate voltage and current mode active fractional circuits. The time dimensional consistency of the fractional derivative terms to the conventional derivative has also been confirmed. These fractional derivative terms have

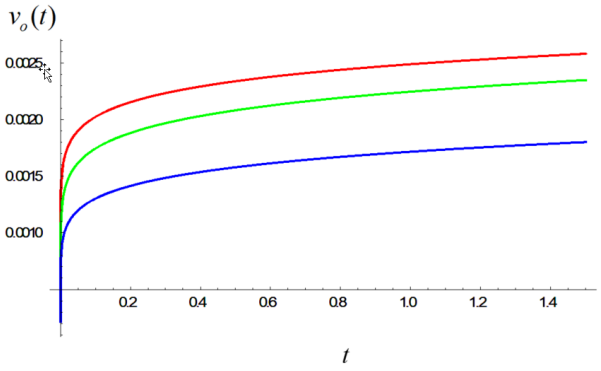

Fig.12: *$v_o(t)$ of the voltage mode circuit with fractional capacitor with t_{PMMA} = 3 μm (red), t_{PMMA} = 4 μm (green) and t_{PMMA} = 6 μm (blue) .*

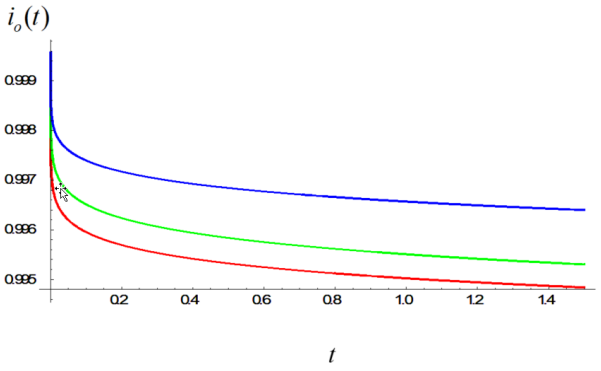

Fig.13: *$i_o(t)$ of the current mode circuit with fractional capacitor with t_{PMMA} = 3 μm (red), t_{PMMA} = 4 μm (green) and t_{PMMA} = 6 μm (blue) .*

been defined in Caputo sense due to its convenience. The resulting time dimensional consistency aware analytical solutions have been determined by using the Laplace transformation based methodology. We have found that there exists dimensional consistency between both sides of the equations of our solutions which cannot be achieved by the solutions proposed in previous work.

By applying different source terms to the obtained solutions, the circuit responses to these source terms have been obtained and the behaviors of both voltage and current mode active fractional circuits have been analyzed. It was found that the behaviors of these fractional circuits become closer to those of their conventional counterparts when α approaches 1. Moreover, the fractional time constants and the pole locations in the F-plane of these circuits have also been determined. For both circuits, we have found that those with lower α are more responsive to the stimulus and their stabilities under the assumed range of α can be guaranteed. Beside these studies, the realizations of these circuits by using the fractional capacitor have also been discussed. This research has been found to be beneficial to the analysis and design of fractional circuits and systems.

ACKNOWLEDGEMENT

The author would like to acknowledge Mahidol University, Thailand, for use of their online database service.

References

[1] J. Rosario, D. Dumur, and J. T. Machado, "Analysis of Fractional-order Robot Axis Dynamics," *IFAC Proceedings*, Vol. 39, No. 11, pp. 367-372, 2006.

[2] M. F. M. Lima, J. A. T. Machado, and M. Crisóstomo, "Experimental Signal Analysis of Robot Impacts in A Fractional Calculus Perspective," *Journal of Advanced Computational Intelligence and Intelligent Informatics*, Vol. 11, No. 9, pp. 1079-1085, 2007.

[3] L. Debnath, "Recent Applications of Fractional Calculus to Science and Engineering," *International Journal of Mathematics and Mathematical Sciences*, Vol. 2003, No. 54, pp. 3413-3442, 2003.

[4] L. Sommacal, P.Melchior, A. Oustaloup, J.-M. Cabelguen, and A. J. Ijspeert, "Fractional Multi-Models of The Frog Gastrocnemius Muscle," *Journal of Vibration and Control*, Vol. 14, No. 9-10, pp. 1415-1430, 2008.

[5] R. L. Magin and M. Ovadia, "Modeling The Cardiac Tissue Electrode Interface Using Fractional Calculus," *Journal of Vibration and Control*, Vol. 14, No. 9-10, pp. 1431-1442, 2008.

[6] Y. Pu, X. Yuan, K. Liao, et al., "A Recursive Two-circuits Series Analog Fractance Circuit For Any Order Fractional Calculus," *Proceedings of SPIE ICO20 Optical Information Processing*, pp. 509-519, 2006.

[7] B. T. Krishna and K. V. V. S. Reddy, "Active and Passive Realization of Fractance Device of Order 1/2," *Active and Passive Electronic Components*, Vol. 2008, pp. 1-5, 2008.

[8] Z.-Z. Yang and J.-L. Zhou, "An Improved Design for The IIR-type Digital Fractional Order Differential Filter," *Proceedings of the International Seminar on Future BioMedical Information Engineering (FBIE '08)*, pp. 473-476, 2008.

[9] R. Panda and M. Dash, "Fractional Generalized Splines and Signal Processing," *Signal Processing*, Vol. 86, No. 9, pp. 2340-2350, 2006.

[10] J. Cervera and A. Baños, "Automatic Loop Shaping in QFT Using CRONE Structures," *Journal of Vibration and Control*, Vol. 14, No. 9-10, pp. 1513-1529, 2008.

[11] G.W. Bohannan, "Analog Fractional Order Controller in Temperature and Motor Control Applications," *Journal of Vibration and Control*, Vol. 14, No. 9-10, pp. 1487-1498, 2008.

[12] R. Caponetto, G. Dongola, L. Fortuna, I. Petras, *Fractional Order System-Modeling and Control*

Applications,World Scientific Publishing, Singapore, 2010.

[13] A.G. Radwan, A.M. Soliman, A.S. Elwakil and A. Sedeek, "On The Stability of Linear Systems with Fractional Order Elements," *Chaos, Solitons and Fractals*, Vol. 40, No 5. pp. 2317-2328, 2009.

[14] A.G. Radwan, A.M. Soliman and A.S. Elwakil, "First-Order Filters Generalized to The Fractional Domain," *Journal of Circuits, Systems, and Computers*, Vol. 17, No. 1,pp. 55-66, 2008.

[15] A.G. Radwan, A.S. Elwakil and A.M. Soliman, "On The Generalization of Second Order Filters to The Fractional Order Domain," Journal of Circuits, Systems, and Computers , Vol.18, No. 2, pp. 361-386, 2009.

[16] T.J. Freeborn, B. Maundy and A.S. Elwakil, "Field Programmable Analogue Array Implementation of Fractional Step Filters," *IET circuits, devices & systems*, Vol. 4, No. 6, pp. 514-524, 2010.

[17] A.G. Radwan, A.S. Elwakil and A.M. Soliman, "Fractional-order Sinusoidal Oscillator: Design Procedure and Practical Examples," *IEEE Transactions on Circuits and Systems I: Regular Papers*, Vol. 55, No.7, pp. 2051-2063, 2008.

[18] D. Mondal and K. Biswas, "Performance Study of Fractional Order Integrator Using Single-component Fractional Order Element," *IET circuits, devices & systems*, Vol.5, No. 4, pp. 334-342, 2011.

[19] M. Guia, F. Gomez, and J. Rosales, "Analysis on The Time and Frequency Domain for The RC Electric Circuit of Fractional Order," *Central European Journal of Physics*, Vol. 11, No. 10, pp. 1366-1371, 2013.

[20] A. A. Rousan, N. Y. Ayoub, F. Y. Alzoubi et al., "A Fractional LC-RC Circuit," *Fractional Calculus & Applied Analysis*, Vol. 9, No. 1, pp. 33-41, 2006.

[21] P. V. Shah, A. D. Patel, I. A. Salehbhai, and A. K. Shukla, "Analytic Solution for the Electric Circuit Model in Fractional Order," *Abstract and Applied Analysis*, Vol. 2014, pp. 1-5, 2014.

[22] R. Banchuin and R. Chaisricharoen, "The analysis of active circuit in fractional domain," *Proceedings of the 2018 ECTI Northern Section Conference on Electrical Electronics, Computer and Telecommunications Engineering (ECTI-NCON 2018)*, pp. 25-28, 2018.

[23] R. Banchuin and R. Chaisricharoen, "Time Domain FDE Based Analysis of Active Fractional Circuit," *Proceedings of the 2018 International Conference on Digital Arts, Media and Technology (ICDAMT 2018)*, pp. 25-28, 2018.

[24] J.F. Gómez-Aguilara, J.J. Rosales-Garcíab, J.J. Bernal-Alvaradoa, T. C?rdova-Fragaa and R. Guzmn-Cabrerab, "Fractional Mechanical Oscillators," *Revista Mexicana de Física*, Vol. 58, No. 8, pp. 348-352, 2012.

[25] G.-A. J. Francisco1, R.-G. Juan3, G.-C. Manuel and R.-H. J. Roberto, "Fractional RC and LC Electrical Circuits," *Ingeniería, Investigación y Tecnología*, Vol. 15, No. 2, , pp. 311-319, 2014.

[26] F. Gómez, J. Rosales and M. Gua, "RLC Electrical Circuit of Non-integer Order," *Central European Journal of Physics*, Vol.11, No. 10, pp 1361-1365

[27] A. Fabre, "Insensitive Voltage-mode and Current-mode Filters from Commercially Available Transimpedance Opamps," *IEE Proceedings G (Circuits, Devices and Systems)*, Vol. 140, No. 5, pp. 319-321, 1993.

[28] J. Mahattanakul and C. Toumazou, "Current-mode Versus Voltage-mode Gm-C Biquad Filters: What the theory says," *IEEE Transactions on Circuits and Systems II: Analog and Digital Signal Processing*, Vol. 45, No. 2, pp. 173-186, 1998.

[29] I. Podlubny, "Fractional Differential Equations," *Vol. 198 of Mathematics in Science and Engineering*, Academic Press, New York, 1999.

[30] A. Atangana and A. Secer, "A Note on Fractional Order Derivatives and Table of Fractional Derivatives of Some Special Functions," *Abstract and Applied Analysis*, Vol. 2013, pp. 1-8, 2013.

[31] E. Kreyszig, *Advanced Engineering Mathematics*, John Wiley and Sons, Inc., New York, 1999.

[32] A. M. Mathai and H. J. Haubold, *Special Functions for Applied Scientists*, Springer, New York, 2010.

[33] T. Deliyannis, Y. Sun, and J.K. Fidler, *Continuous - Time Active Filter Design*, CRC Press, Florida, 1999.

[34] E. W. Weisstein, "Regularized Hypergeometric Function," *MathWorld-A Wolfram Web Resource.*

[35] B. Dwork, *Generalized Hypergeometric Functions*, Clarendon Press, Oxford,1990.

[36] M.S. Semary, A.G. Radwan and H.N. Hassan, "Fundamentals of Fractional-order LTI Circuits and Systems: Number of Poles, Stability, Time and Frequency Responses," *International Journal of Circuit Theory and Applications*, Vol. 44, No. 12, pp. 2114-2133, 2016.

[37] A. Agambayev, S. Patole, M. Farhat, A. Elwakil, H. Bagci and K. N. Salama, "Ferroelectric Fractional-Order Capacitors," *ChemElectroChem*, Vol. 4, No. 11, pp. 2807-2813, 2017.

[38] D. A. John, S. Banerjee, G. W. Bohannan and K. Biswas, "Solid-state Fractional Capacitor Using MWCNT-epoxy Nanocomposite," *Applied Physics Letters*, Vol. 110, No. 16, pp. 163504-1-163504-5, 2017.

[39] C. Halijak, "An RC Impedance Approximant to

$(1/s)^{1/2}$," *IEEE Transactions on Circuit Theory*, Vol. 11, No. 4, pp. 494-495, 1964.

[40] J. Valsa and J. Vlach, "RC Models of A Constant Phase Element," *International Journal of Circuit Theory and Applications.*, Vol. 41, No. 1, pp. 59-67, 2013.

[41] R. Banchuin, "Novel Expressions for Time Domain Responses of Fractance Device," *Cogent Engineering*, Vol. 4, No. 1, pp. 1-28, 2017.

[42] T. J. Freeborn, B, Maundy and A.S. Elwakil, "Measurement of Supercapacitor Fractional-order Model Parameters From Voltage-excited Step Response," *IEEE Journal on Emerging and Selected Topics in Circuits and Systems*, Vol. 3, No. 3, pp. 367-376, 2013.

[43] S. Das, K. Biswas and B. Goswami, "Study of The Parameters of A Fractional Order Capacitor," *Proceedings of INDICON 2015 Annual IEEE India Conference*, pp. 1-5, 2015.

Rawid Banchuin received the B.Eng. degree in electrical engineering from Mahidol University, Bangkok, Thailand in 2000, the degree of M.Eng. in computer engineering and Ph.D. in electrical and computer engineering from King Mongkuts University of Technology Thonburi, Bangkok, Thailand in 2003 and 2008 respectively. At the present, he is an assistant professor of the Graduated School of Information Technology and Faculty of Engineering, Siam University, Bangkok, Thailand. His research interests are computation and mathematics in electrical and electronic engineering especially the fractional order and memristive devices, circuits and systems.

Roungsan Chaisricharoen received B.Eng., M.Eng. and Ph.D. degrees from the department of computer engineering, King Mongkuts University of Technology Thonburi, Bangkok, Thailand. He is an assistant professor at the school of information technology, Mae Fah Luang University, Chiang Rai, Thailand. His research interests are computational intelligence, analog circuits and devices, wireless networks and optimization techniques. At the present, Asst. Prof. Dr. Roungsan Chaisricharoen is a member of ECTI board committee, public relations personal of ECTI.

APPENDIX

Since many crucial specific functions and variables have been introduced in this work, a table of their notations will be shown here for the convenience of readers who may not be familiar with them.

Table 1: *Notations of crucial specific functions and variables.*

C_α	Pseudo capacitance
$\frac{d^\alpha}{dt^\alpha}$	α^{th} order Fractional c
F	Fractional power complex variable
$E_\alpha(\ )$	Mittag-Leffler function
$E_{\alpha,\beta}(\ )$	Generalized Mittag-Leffler function
${}_p\tilde{F}_q(\ ;\ ,\ ;\ )$	Regularized hypergeometric function
${}_pF_q(\ ;\ ,\ ;\ )$	Generalized hypergeometric function
t_{PMMA}	Thickness of polymethyl methacrylate coating film on the electrode
$T_{\alpha i}$	Fractional time constant of the current mode active fractional circuit
$T_{\alpha v}$	Fractional time constant of the voltage mode active fractional circuit
α	Order of fractional derivative
$\Gamma(\ )$	Gamma function
σ	Fractional time component
σ_i	Fractional time component of the current mode circuit
σ_v	Fractional time component of the voltage mode circuit